GEEA
Research article
Geochemistry: Exploration, Environment, Analysis
Published Online First
https://doi.org/10.1144/geochem2017-008

Identifying ore-related anomalies using singularity mapping of stream sediment geochemical data, a case study of Pb mineralization in the Qinling region, China

Qin-Ping Tan[1,2,3*], Xueqiu Wang[1,3*], Yong Xia[2], Qingqing Liu[1,3] & Jian Zhou[1,3]

[1] Key Laboratory of Geochemical Exploration, Institute of Geophysical and Geochemical Exploration, Langfang, Hebei 065000, China
[2] State Key Laboratory of Ore Deposit Geochemistry, Institute of Geochemistry, Chinese Academy of Sciences, Guiyang, Guizhou 550081, China
[3] UNESCO International Centre on Global-scale Geochemistry, Langfang, Hebei 065000, China
* Correspondence: 565310821@qq.com; wangxueqiu@igge.cn

Abstract: The Qinling region is located in the central part of the China mainland and carries abundant mineral resources. Stream sediment and rock geochemical data of the Qinling region collected from the Regional Geochemistry-National Reconnaissance Project of China and the China Geochemical Baselines Project, respectively, were used to identify the Pb distribution pattern and to explain the geogenic sources of geochemical anomalies. The singularity mapping technique was applied to extract local Pb ore-related geochemical anomalies from complicated geochemical backgrounds. One geochemical mega-province, one geochemical province, and three regional anomalies were delineated in a Pb geochemical map of the Qinling region. The spatial distributions of the regional anomalies are all consistent with that of known Pb metallogenic districts, but only local high anomalous areas in the geochemical province and mega-province contain economic Pb ore deposits. Regions with singularity indices of less than 1.884 occupy 2.70% of the total study area, but contain 60% of the total known Pb deposits in a Pb singularity map of the Qinling region. Targets delineated in the Pb singularity map not only highlighted known areas of Pb mineralization, but also identified areas of high potential for undiscovered ore deposits in the Qinling region.

Keywords: Qinling; stream sediment; rock; singularity mapping; geochemical anomaly

Received 8 February 2017; **revised** 20 October 2017; **accepted** 15 December 2017

Geochemical anomalies can provide important clues to the presence of ore deposits, and they play an increasingly significant role for mineral exploration. In China, 817 new ore deposits were discovered in follow-up exploration of geochemical anomaly targets between 1981 and 2000 (Wang *et al.* 2016). Identifying geochemical anomalies from background to delineate potential areas for detailed investigation is a basic task in exploration geochemistry (Cohen *et al.* 2010). The usual and most widely used method for identifying geochemical anomalies is setting threshold values (Hawkes & Webb 1962) that contain the upper and lower limits of the background range. Areas with concentrations outside of this range are defined as anomalies.

Various statistical methods have been applied to identify geochemical thresholds, such as mean ± two standard deviations, 85th percentile, histograms, probability graphs, box-plots, and quantile–quantile (Q-Q) plots (Hawkes & Webb 1962; Sinclair 1974; Govett *et al.* 1975; Miesch 1981; Stanley & Sinclair 1989). In the Qinling region, a traditional statistical approach based on the mean ± two standard deviations has been used to delineate nested hierarchy gold anomalies and identified geochemical thresholds of 4 μg/kg for local concentration centres, 3 μg/kg for regional anomalies, and 2 μg/kg for geochemical provinces (Wang *et al.* 2013*a*; Ye *et al.* 2014). However, most standard statistical techniques are based on the frequency distribution of geochemical data and neglect the spatial variability of geochemical patterns. In addition, areas with different rock compositions, or that have undergone different geological and geomorphological processes, result in different geochemical thresholds. Weak anomalies in areas with low background levels, or weak anomalies superimposed on high background levels, are difficult to distinguish (Cheng 2012). Application of a global threshold value to delineate anomalies is not reliable in areas with a complex geological background. Several frequency-space-based interpolation methods have been suggested to account for the spatial dependence of exploration geochemical data, such as inverse distance-weighting and kriging (Lam 1983; Zimmerman *et al.* 1999). Although these interpolation methods acknowledge the spatial dependence of element concentrations, they invariably lead to the smoothing-out of anomalous values and ignore the irregularity and local variation of geochemical anomalies (Cheng 2007; Zuo & Wang 2016).

Recent studies of geochemical patterns at different spatial scales have shown that self-similarity or self-affinity are fundamental properties of geochemical data (e.g. Bölviken *et al.* 1992; Carranza 2010; Afzal *et al.* 2011; Agterberg 2012; Zuo & Wang 2016). The spatial statistical distribution of geochemical data can be characterized by self-similarity (Mandelbrot 1983), and geochemical anomalies caused by non-linear geological processes obey fractal or multifractal theory. Therefore, methods that synchronously consider the frequency and spatial variation of data have been developed to identify geochemical anomalies, such as fractal or multifractal models (Cheng *et al.* 2000; Cheng 2007; Zuo *et al.* 2009) and local neighbourhood statistics (Luz *et al.* 2014; Zuo 2014). A spatial singularity mapping technique based on fractal and multifractal theory was proposed by Cheng (1997, 2006, 2007, 2012) to measure the local structural properties of geochemical maps. Singularity indices are linearly related to logarithmically transformed element concentrations (Agterberg 2012), and they can be used to measure the small-scale nugget effect caused by

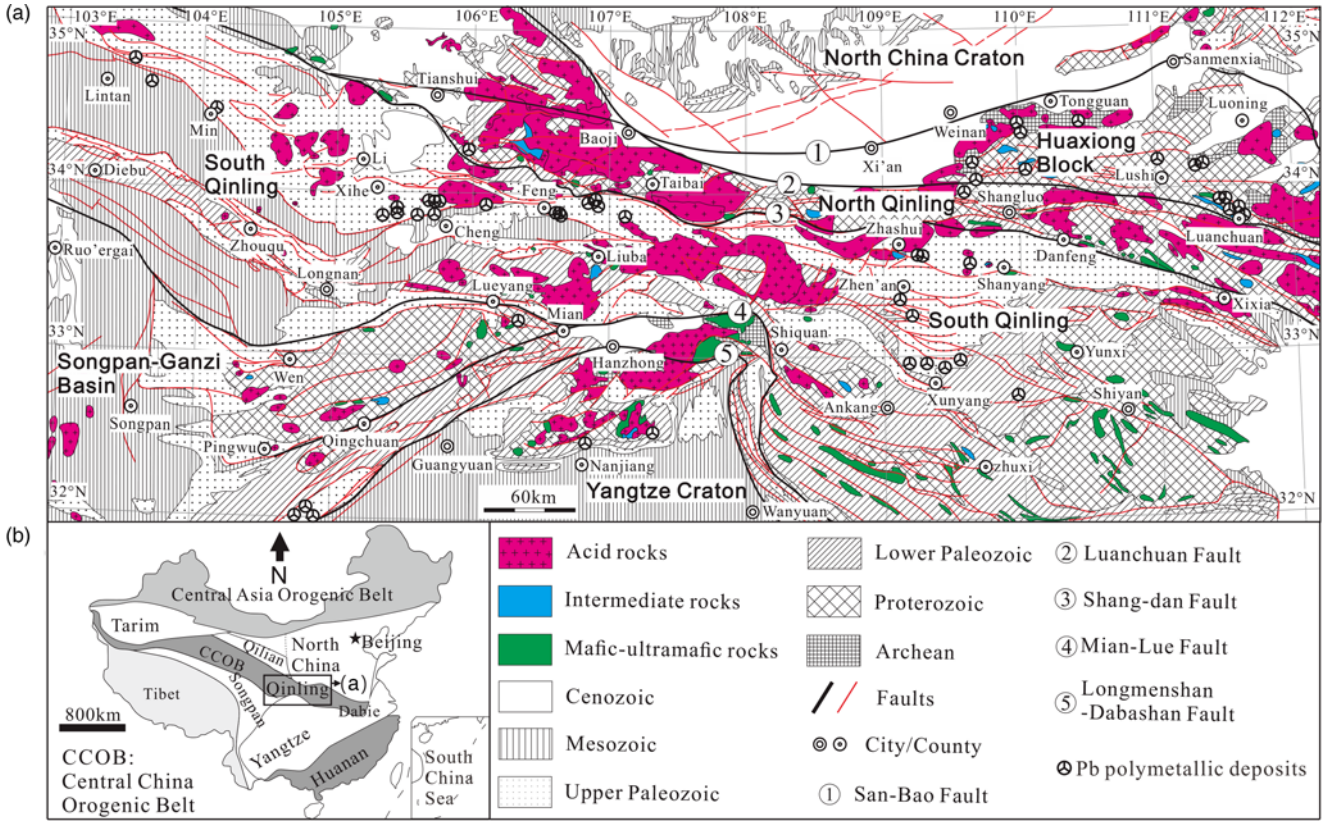

Fig. 1. (**a**) Geological map of the Qinling region showing the major tectonic units, rock units, and Pb polymetallic deposits (modified after the National Geological Archives of China, http://en.ngac.org.cn/). (**b**) Schematic tectonic map of China showing the location of the Qinling region (modified after Chen & Santosh 2014).

measurement error and microscopic randomness. Zuo *et al.* (2015) proposed a modified algorithm for estimating singularity indices, as the original algorithm was found to be influenced by background values. The singularity mapping technique has been demonstrated as a powerful tool for recognizing weak geochemical anomalies in complex geological settings or in areas covered by overburden (e.g. Ali *et al.* 2007; Xie *et al.* 2007; Cheng & Agterberg 2009; Zuo *et al.* 2009; Bai *et al.* 2010; Sun *et al.* 2010; Arias *et al.* 2012; Cheng 2012; Liu *et al.* 2013; Zhao *et al.* 2015; Yang *et al.* 2016; Liu *et al.* 2017).

In this study, the Qinling region was chosen as a case study region because it is known to host clusters of Pb polymetallic deposits and has good potential for the discovery of more. Stream sediment geochemistry data collected from the Regional Geochemistry-National Reconnaissance Project of China (GNRP) were used to identify the Pb distribution pattern in the Qinling region. Rock geochemistry data of the Qinling region, collected from the China Geochemical Baselines Project (CGB), aided in the interpretation of geogenic sources of geochemical anomalies. The singularity mapping technique was applied to extract local Pb ore-related geochemical anomalies from complicated geochemical backgrounds in the Qinling region.

Geological setting

The Qinling Orogenic Belt, an important part of the Central China Orogenic Belt, is located between the North China Craton and the Yangtze Craton (Fig. 1a) (Meng & Zhang 2000; Dong & Santosh 2016). The Qinling Orogenic Belt connects the Qilian Orogenic Belt to the NW, the Songpan–Ganzi Basin to the SW, and the Dabie–Sulu Orogenic Belt to the east (Chen & Santosh 2014). It is bounded by the San–Bao Fault to the north and the Mian–Lue Fault to the south. The Luanchuan Fault and the Shang–Dan Fault subdivide the Qinling Orogenic Belt into the Huaxiong Block, the North Qinling Orogenic Belt, and the South Qinling Orogenic Belt (Zhang *et al.* 1995). The major tectonic units, rock units, and Pb polymetallic deposits are shown in the geological map of the Qinling region (Fig. 1b).

Mineral deposits in the Qinling region show northward trends, with epizonogenic hydrothermal deposits restricted to the south and magmatic and metamorphic hydrothermal deposits mainly in the north. Sedimentary exhalative (SEDEX)-type Pb–Zn deposits reworked by hydrothermal processes are hosted in Devonian clastic carbonate–barite–chert strata in the South Qinling Orogenic Belt (Ma *et al.* 2004), such as the Yeshuihe, the Changba, the Luoba, and the Er'lihe Pb–Zn deposits. The Huaxiong Block are dominated by orogenic-type or magmatic hydrothermal Pb–Zn–Ag deposits (Chen & Santosh 2014). Most known Pb–Zn–Ag deposits in the Huaxiong Block are porphyry and porphyry–skarn types with mineralization occurring within granite porphyry intrusions and outer contact zones (Zhu *et al.* 2010; Wang *et al.* 2013*b*), such as the Lengshuibeigou and Bailugou Pb–Zn–Ag deposit.

Methods

Singularity has been defined as a special phenomenon in a geological field caused by anomalous energy release or material accumulation occurring within narrow spatial-temporal intervals (Cheng 2007). The phenomenon is commonly characterized by scale invariance and self-similarity properties based on non-linear and multifractal theory. For a geochemical distribution map, the singularity can be described as a power–law relationship between a given area A (ε) and the average concentration X [A(ε)]:

$$X[A(\varepsilon)] = c\varepsilon^{\alpha-2}, \quad (1)$$

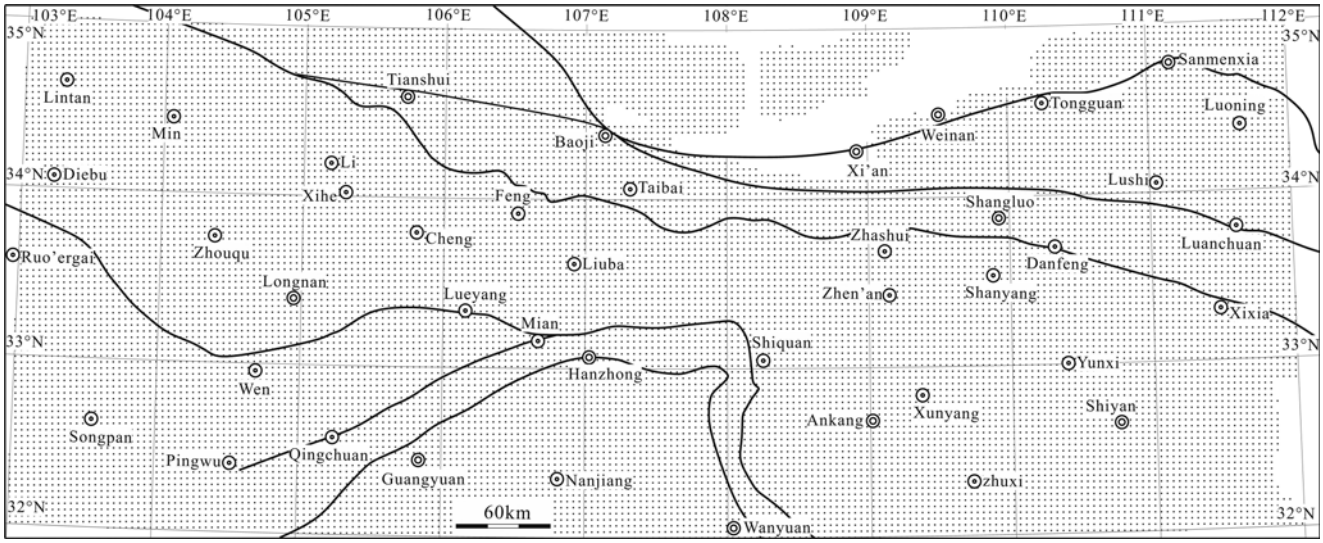

Fig. 2. Locations of calculated stream sediment data in the Qinling region. The raw geochemical data contained 64 066 stream sediment samples with a density of approximately one sample per 4 km^2. The average concentration of Pb was calculated for each 4 × 4 km grid square (approximately one sample per 16 km^2) to given 17 200 grid points. The average was placed at the centre point of each grid square.

where c is a constant, ε is a normalized distance measure such as window size, and α is the singularity index. In a 2-dimension geochemical map, α varies roughly around two indicating a normal distribution. The positive singularity ($\alpha < 2$) usually corresponds to 'enriched' or elevated element concentration values, whereas the negative singularity ($\alpha > 2$) corresponds to 'depleted' values.

A window-based method (Cheng 2007; Zuo *et al.* 2009; Sun *et al.* 2010) was used to estimate the α-values from a geochemical map. First, for a given sampling point on a map, define a set of sliding windows with variable window sizes ($\varepsilon_1 < \varepsilon_2 < \varepsilon_3 \ldots < \varepsilon_n$). Secondly, calculate the average concentration X [A(ε_i)] (i = 1, …, n) in each window area A (ε_i). The values of X [A(ε_i)] will show a linear trend with window size ε_i on log–log graph or Log X [A(ε)] = c + (α − 2) Log(ε). The slope of the straight line is considered to be an estimate of α − 2.

A computer software package (GeoDAS GIS) was used (Cheng 2000) for mapping the α-values of the stream sediment Pb concentrations in the Qinling region. The most important choice that needs to be made is the selection of an appropriate window size for the calculation of the α-values. The optimum window size is usually defined experimentally. We set square windows with half window sizes to 2, 6, 10, 14, 18, and 22 at 4-km intervals. The singularity theory has been introduced and applied in many studies (e.g. Ali *et al.* 2007; Xie *et al.* 2007; Cheng & Agterberg 2009; Zuo *et al.* 2009; Bai *et al.* 2010; Sun *et al.* 2010; Arias *et al.* 2012; Cheng 2012; Liu *et al.* 2013; Zhao *et al.* 2015; Yang *et al.* 2016; Liu *et al.* 2017), and more detailed explanations can be found in Cheng (2007).

To quantitatively measure the spatial correlation between the distribution of α-values and the location of known Pb deposits, the weights of evidence method was applied. This method provides a Student's t-value that measures the significance of spatial correlation between point features and polygons (Bonham-Carter 1994); the larger the t-value, the stronger the spatial correlation. Usually a t-value of 1.96 is accepted as the threshold above which the correlation can be considered statistically significant (Cheng 2007; Zuo *et al.* 2009). The Student's t-value can be estimated as

$$t = C/S(C), \quad (2)$$

where $C = W^+ - W^-$, and S(C) is the standard deviation of C. W^+ and W^- are the weights when evidential patterns (e.g. geochemical anomalies) are present and absent, respectively.

Data

This study utilized geochemical data from 64 066 stream sediment samples covering the Qinling region [32 to 35° N, 103 to 112° E], with a density of approximately one sample per 4 km^2. The data were collected under the GNRP, which was initiated in January 1979 and includes stream sediment sampling across 5.17 million km^2 of territory with multi-element analyses of 39 major, minor, trace, and sub-trace elements. Details of sampling and chemical analysis are given in Xie *et al.* (1997). Concentrations of Pb in the stream sediments were determined by X-ray fluorescence spectrometry under strict laboratory analytical quality control. The average concentration of Pb was calculated for each 4 × 4 km grid square (approximately one sample per 16 km^2) to given 17 200 grid points. The average was placed at the centre point of each grid square (Fig. 2). We used the stream sediment geochemical data for the calculated geochemical concentrations of Pb.

We used an additional 588 rock samples in the Qinling region (Fig. 3) from the CGB to aid in the interpretation of the geogenic sources of elements. The CGB was launched in 2008, and sampling was completed in 2012. Its purpose was to document the abundance and spatial distribution of chemical elements covering all of China. Details of sampling and chemical analysis can be found in Wang & the CGB Sampling Team (2015). Typical samples represent the main types of rocks including sedimentary, magmatic, and metamorphic rocks from different geological times. Sampling for the rocks in the CGB avoided areas of mineralized alteration. Concentrations of Pb in the rocks were determined by inductively coupled plasma mass spectrometry under strict laboratory analytical quality control.

Results and discussion

Statistical characteristics of Pb in the stream sediments and rocks

Histograms and Q-Q plots of logarithmic Pb concentrations in the stream sediments (Fig. 4a and b, respectively) and rocks (Fig. 4c and d, respectively) and statistical parameters are summarized in Figure 4. The skewness and kurtosis of the logarithmic Pb concentrations in the stream sediments are 0.89 and 4.95, respectively. This indicates that the data are positively skewed containing large positive tailing values with excess kurtosis, and the

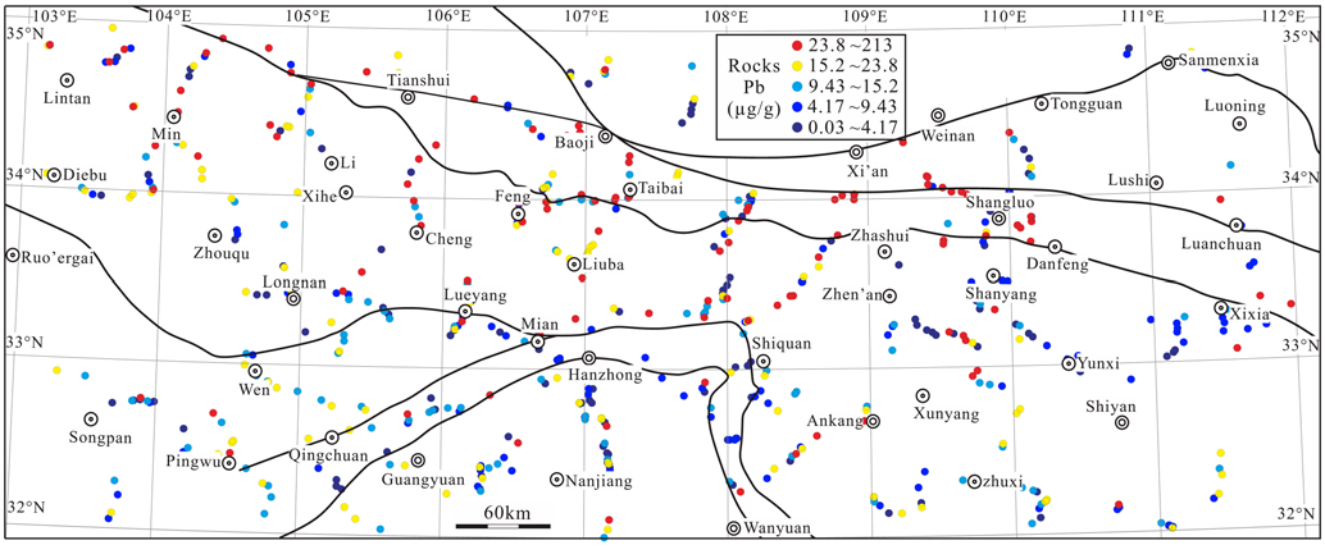

Fig. 3. Locations of 588 rock samples marked by colour dots in the Qinling region. The five colour dot classes are based on the following percentiles of raw data: <20% (dark blue), ≥20 to <40% (blue), ≥40 to <60% (light blue), ≥60 to ≤80% (yellow), and >80% (red) Pb content.

data do not follow a normal distribution (as shown by the histogram, Fig. 4a, and Q-Q plot, Fig. 4b). The skewness and kurtosis of the logarithmic Pb concentrations in the rocks are −1.21 and 2.60, respectively, indicating that the data have negative skewness and normal kurtosis and do not fully follow a normal distribution (as shown by the histogram, Fig. 4c, and Q-Q plot, Fig. 4d). In addition, the histogram of the logarithmic Pb concentrations has a bimodal pattern for the stream sediments (Fig. 4a) and a multimodal pattern for the rocks (Fig. 4c). These statistical characteristics imply that the Qinling region contains multiple geochemical settings and has undergone various geological processes causing complex ore-forming processes throughout geological history. Some of the values, especially the extremely high ones, may satisfy fractal or multifractal distributions.

Spatial distribution pattern of Pb in the stream sediments and rocks

Anomaly areas with high stream sediment Pb concentrations (>41.9 μg/g, 85th percentile), represented by orange red to dark red shading, are delineated in Figure 5. In total, five anomalous districts can be visually recognized. The first district (Pb1) with an area of approximately 80 536 km^2 is mainly located in the middle of the Qinling region, including the areas of the Xi'an, Baoji, Hanzhong, Ankang, and Weinan cities. The second district (Pb2), with an area of 4121 km^2, is situated between the Luoning and Luanchuan counties. The third district (Pb3), with an area of 396 km^2, is between the Feng County and the Tianshui City. The fourth district (Pb4), with an area of 558 km^2, is located between the

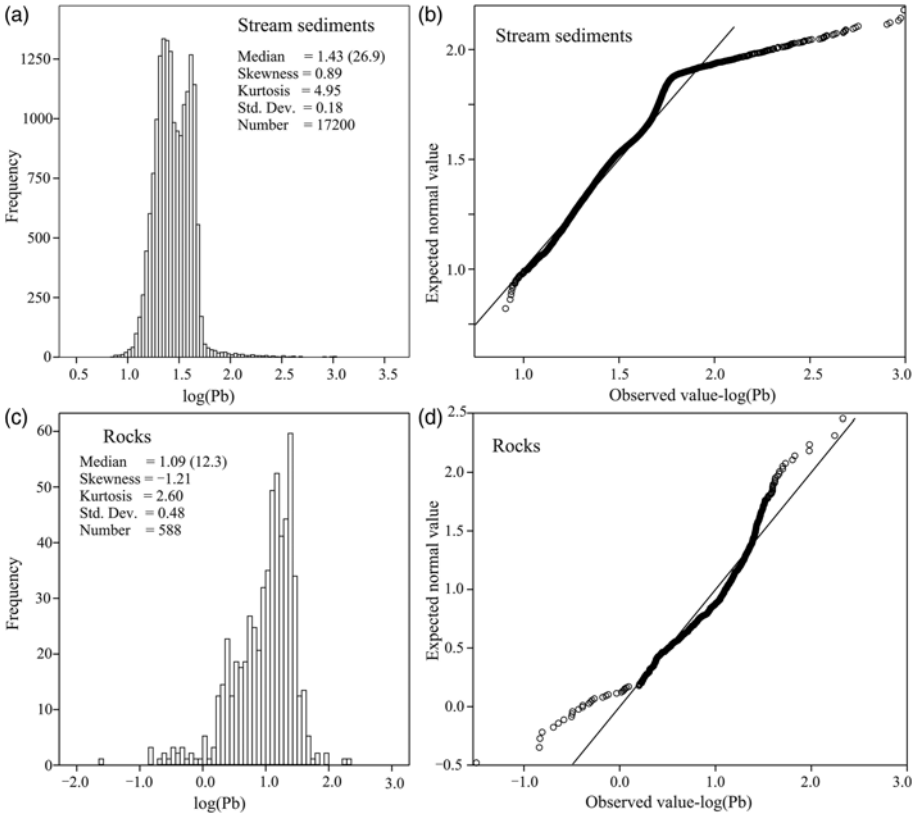

Fig. 4. Histograms and Q-Q plots of logarithmic Pb concentrations in the stream sediments (**a** and **b**, respectively) and rocks (**c** and **d**, respectively).

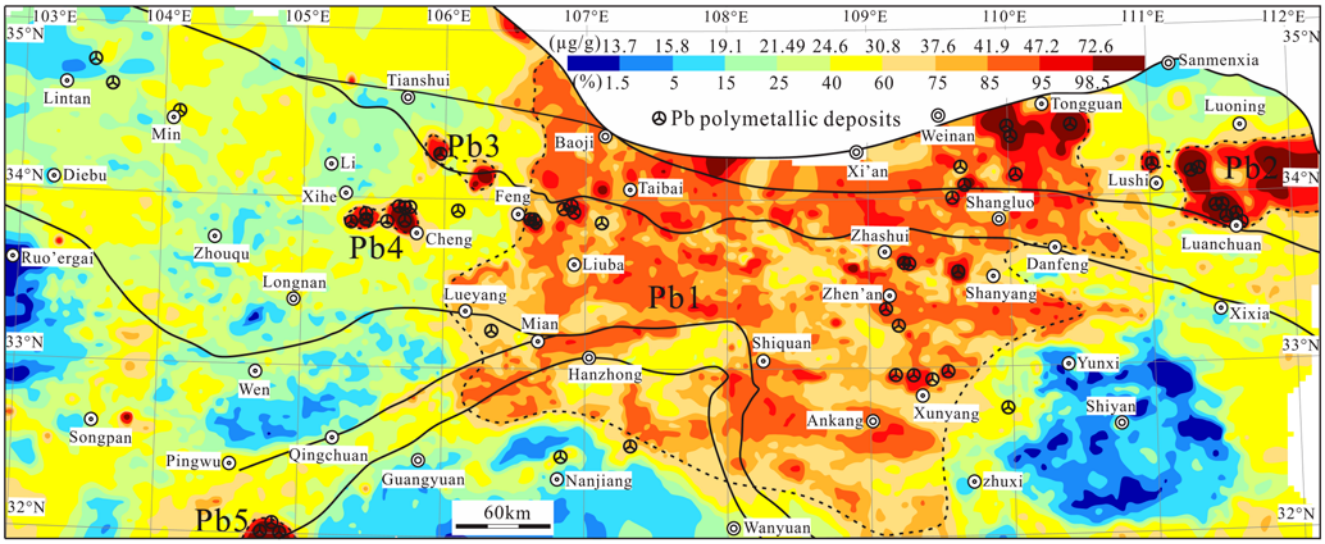

Fig. 5. Spatial distribution map of the stream sediment Pb concentrations (μg/g) in the Qinling region. The colour classes are based on the following percentiles of raw data: 1.5, 5, 25, 40, 60, 75, 85, 95, and 98.5% Pb content.

Cheng and Xihe counties. The fifth district (Pb5), with an area of 350 km^2, is situated at the south of the Pingwu County.

Xie & Yin (1993) summarized the classification of geochemical patterns from local anomalies (0.1 to 1 × n km^2), regional anomalies (10 to 100 × n km^2), geochemical provinces (1000 to 10 000 × n km^2), geochemical mega-provinces (100 000 to 1 000 000 × n km^2) to global pattern (>1 000 000 × n km^2) according to their sizes. Using Xie & Yin's (1993) classification of geochemical patterns, one geochemical mega-province (Pb1), one geochemical province (Pb2), and three regional anomalies (Pb3, Pb4, and Pb5) can be identified in Figure 5.

Local anomalies may be associated with mineralization and/or secondary weathering of existing deposits. Regional anomalies may be associated with the regional syngenetic or epigenetic concentrations of certain elements in rocks during mineral-forming processes. Many new economic ore deposits were discovered following the identification of regional anomalies during the implementation of China's national geochemical mapping project (Xie & Yin 1993). The spatial distributions of the regional anomalies (Pb3, Pb4, and Pb5) are all consistent with that of known Pb metallogenic districts. For example, Pb3 contains the Guanlinggen Pb–Zn deposit (Liu *et al.* 2008), Pb4 contains the Changba Pb–Zn deposit (Ma *et al.* 2004), and Pb5 contains the Qingshan Pb–Zn deposit (Zhou *et al.* 2013).

The term geochemical province, first defined by Hawkes & Webb (1962), is a relatively large segment of the Earth's crust that has a chemical composition significantly different from the average (Rose *et al.* 1979). Geochemical provinces, as well as geochemical mega-provinces and global patterns, may be related to large-scale crustal units characterized by common features of geological and geochemical evolution expressed in chemical composition of the constituent geological complexes. In Figure 3, rocks around the Pb1 geochemical mega-province mostly show high Pb concentrations (>23.8 μg/g, 80th percentile) (marked by red dots). Statistical parameters and boxplots of the Pb concentrations in various sedimentary and magmatic rocks are shown in Table 1 and Figure 6, respectively. Metamorphic rocks were classified into sedimentary or magmatic according to their original rocks. The Intermediate (δ), Acid (γ), Archaean (Ar), Silurian (S), Jurassic (J), Cretaceous (K), and Cenozoic (E) rocks display high median Pb concentrations (>13.3 μg/g, the median of all rock samples). In Figure 1, the Intermediate and Acid rocks are mostly distributed in the Huaxiong Block, the North Qinling Orogenic Belt, and the middle-west of the

Table 1. *Statistical parameters for Pb (in ug/g) in various sedimentary and magmatic rocks in the Qinling region*

			Percentile (%)					
Sample types	N	Min.	25	50	75	Max.	Mean	Standard deviation
Ultramafic-mafic rocks (Σ)	18	1.61	2.52	4.36	8.00	20.1	6.08	4.95
Intermediate rocks (δ)	30	4.47	8.60	16.5	24.8	39.3	17.0	9.25
Acid rocks (γ)	65	2.75	15.1	26.5	34.6	213	29.0	26.6
Archaean (Ar)	11	2.39	7.34	25.6	30.0	175	35.3	47.9
Proterzoic (Pt)	89	0.145	4.20	9.51	15.0	67.2	11.1	9.55
Cambrian (Є)	39	0.147	4.20	8.61	14.8	22.5	9.58	5.99
Ordovician (O)	31	0.313	3.92	8.22	16.5	35.3	10.7	8.94
Silurian (S)	53	0.664	12.0	18.6	24.2	39.6	17.9	8.52
Devonian (D)	83	0.155	4.55	11.0	18.3	95.0	13.1	12.9
Carboniferous (C)	39	0.026	2.03	4.17	8.20	38.5	7.32	9.19
Permian (P)	29	0.321	1.78	3.17	20.2	39.5	9.72	11.5
Triassic (T)	44	0.478	6.51	11.1	18.1	95.5	14.0	14.5
Jurassic (J)	20	3.07	8.59	15.7	21.0	32.5	15.6	7.94
Cretaceous (K)	25	10.4	13.5	18.7	24.6	35.1	19.3	6.50
Cenozoic (E)	12	9.82	13.3	20.5	25.5	28.4	19.7	6.33

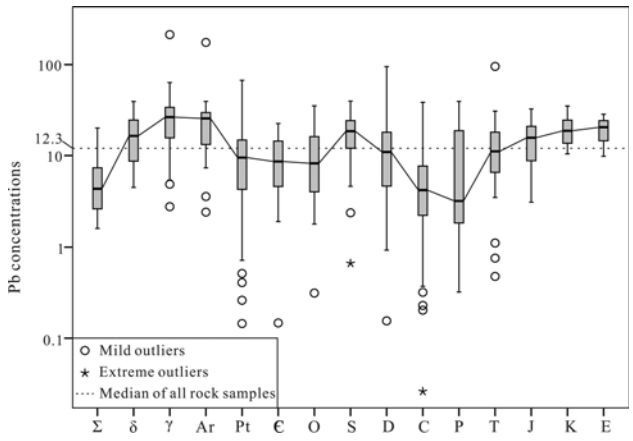

Fig. 6. Boxplots of Pb concentrations in various sedimentary and magmatic rocks in the Qinling region. Box length represents the interquartile range (25th to 75th percentiles), and each box contains the median (thick black line). Σ, Ultramafic-mafic rocks; δ, Intermediate rocks; γ, Acid rocks; Ar, Archaean; Pt, Proterzoic; Є, Cambrian; O, Ordovician; S, Silurian; D, Devonian; C, Carboniferous; P, Permian; T, Triassic; J, Jurassic; K, Cretaceous; E, Cenozoic.

South Qinling Orogenic Belt; the Archaean rocks are mainly located along the south of the San-Bao Fault in the Huaxiong Block; the Silurian rocks are mostly at the south of the South Qinling Orogenic Belt; the Cretaceous and Cenozoic rocks are situated at the NW of the South Qinling Orogenic Belt along the Li, Min, and Lintan counties; the Jurassic rocks are in the Yangtze Craton. Therefore, the geochemical mega-province Pb1 and province Pb2 are mostly associated with large-scale rocks of high Pb concentrations, such as the Intermediate and Acid, Archaean, and Silurian rocks.

Large anomalous areas marked by orange red in Pb1 were caused by large-scale crustal units with high Pb background, and all areas contain no economic Pb deposits. Only the local high anomalous areas shown by dark red in the geochemical province (Pb2) and mega-province (Pb1) contain economic Pb deposits, such as the anomalous areas between the Lushi and Luanchuan counties, between the Weinan and Shangluo cities, between the Zhashui and Shanyang counties, and between the Feng and Taibai counties. Geochemical anomalies are usually induced by rocks with high background levels of elements, mineralization, and secondary dispersion of pre-existing deposits through weathering and erosion (Wang *et al.* 2013*a*; Ye *et al.* 2014). Rocks provide the initial endowment of elements, local mineralization leads to further enrichment, and weathering and erosion lead to secondary dispersion of the ore body from concentration centres. Application of a global threshold value to delineate geochemical anomalies is not reliable in areas with complex geological backgrounds. Thus, distinguishing geochemical anomalies associated with mineralization in regions of high/low geochemical background is vital for exploration geochemistry.

Identifying ore-related Pb anomalies using singularity mapping technique

Frequency histograms and spatial distributions of the α-values are shown in Figures 7a and 8, respectively. The data distribution is unimodal, and most of the α-values are close to 2 (Fig. 7a), implying a greater proportion of non-singular or background values with relatively few $\alpha \neq 2$ (singular values or anomalies). The resulting singularity map (Fig. 8) shows that most of the study area is represented by non-singular element concentrations (α approximately equal to 2, light yellow and blue), corresponding to regions with background geochemical levels. Anomalous areas with extremely high or low α-values generally occupy a small part of the study area.

As shown in Figure 8, the singularity mapping technique can effectively reduce the areas of large-scale positive Pb anomalies and can enhance weak positive anomalies in low geochemical background regions. For example, large areas with high Pb concentrations (shaded in orange red) (41.9 to 47.2 μg/g) are in the middle part of the Qinling region in Figure 5, but these areas only show weak element enrichment in Figure 8 and no economic Pb deposits have been discovered to date. The Pb anomalies in these areas mostly reflect high Pb background. A further example is the Shatan Pb–Zn deposit, located in the north of the Nanjiang County in the Yangtze Craton (Huang & Hou 2016). It is in an area of low Pb concentration (shown in yellow in Fig. 5); however, in the singularity map (Fig. 8), this area shows local Pb enrichment (marked by orange red). Hence, the singularity mapping technique is an efficient method for visually assessing local ore-related anomalies, where the element concentration is significantly different from that of a large background area.

Most of the known Pb deposits in the Qinling region are spatially coincident with anomalous areas where $\alpha < 2$ in the singularity map (Fig. 8). Areas from orange red to dark red shading that represent strong Pb enrichment contain most of the known Pb deposits, yellow-shaded areas show weak Pb enrichment with fewer known Pb deposits, and light to dark blue areas show Pb depletion with the least number of known Pb deposits. The calculated t-values (illustrated in Fig. 7b) show that as the α-value increases, the t-value first increases and then decreases. A maximum t-value of 13.85 is reached at the optimum threshold α-value of 1.884. Areas with α-values below the threshold (marked by orange to dark red) have the strongest spatial correlation with the locations of known Pb deposits (Fig. 8). Regions with α-values ≤1.884 occupy 2.70% of the total study area, but contain 60% of the total known Pb deposits.

The formation of a deposit is a geological singularity and is not necessarily related to the regional abundance of geochemical

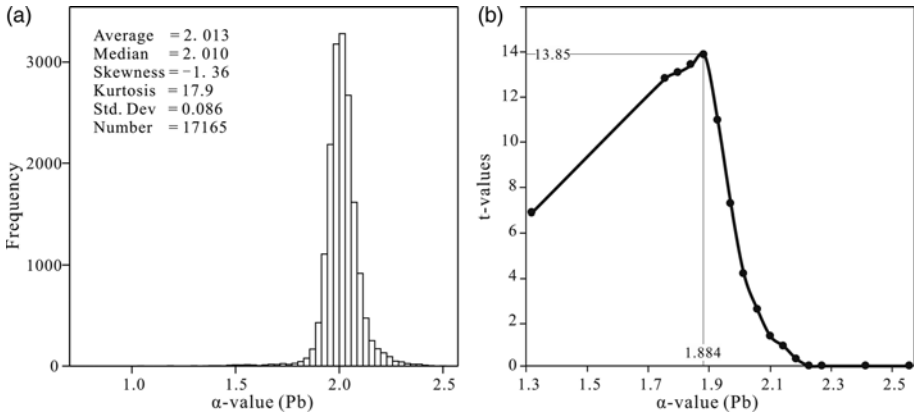

Fig. 7. (**a**) Histogram of calculated α-values of the stream sediment Pb concentrations. (**b**) Student's t-value calculated by the weights of evidence method for measuring spatial correlation between locations of known Pb mineral deposits and areas with α-values below variable thresholds, as expressed along the x-axis. The highest t-value (13.85) is reached at $\alpha = 1.884$.

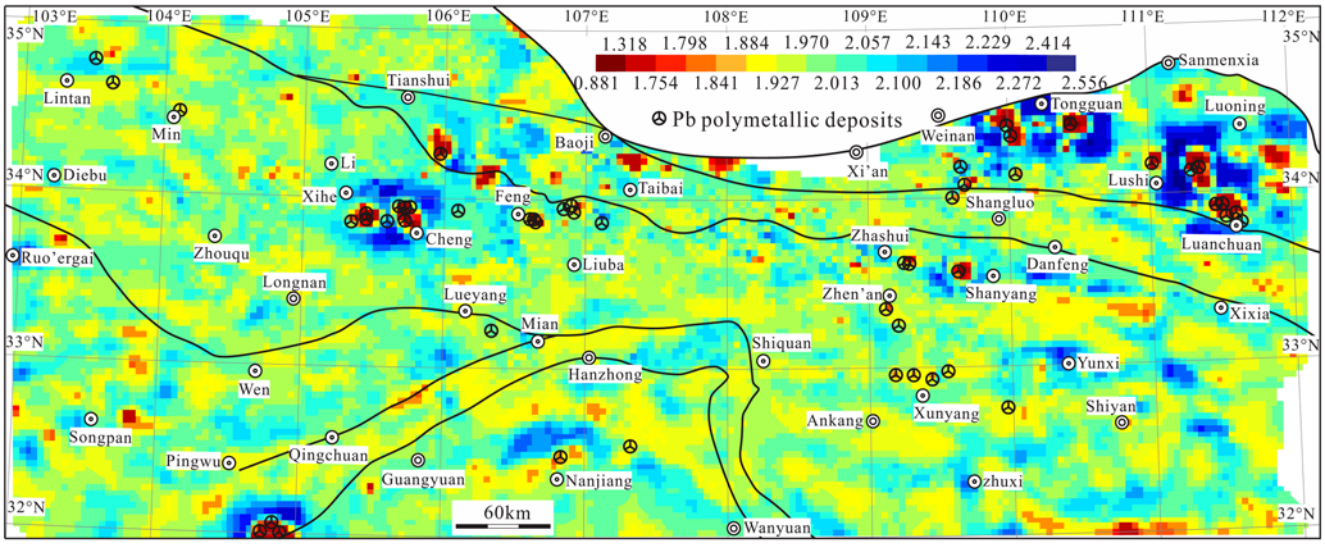

Fig. 8. Raster map showing α-values of the stream sediment Pb concentrations estimated using the window-based method. The orange to dark red areas with $\alpha < 1.884$ occupy 2.7% of the total study area but contain 60% of the total Pb deposits.

elements (Cheng 2007). Anomalous patterns created by mineralization processes are often different in spatial and frequency properties. Thus, singularity analysis is important for extracting ore-related anomalies from complicated geochemical backgrounds. The singularity mapping method can provide new information that complements results based on the original element concentrations, and it can quantify the properties of enrichment and depletion caused by mineralization. Distribution of the stream sediment Pb α-values obtained from singularity analysis helped delineate anomalies caused by mineralization and helped predict locations of undiscovered mineral deposits in the Qinling region. Many areas marked from orange red to dark red in Figure 8 have been identified as having potential economic Pb deposits and are awaiting follow-up exploration.

Conclusions

The Qinling region, China, contains multiple geochemical settings and has undergone various geological processes causing complex ore-forming processes throughout its geological history. Geochemical anomalies delineated by a global threshold value are not reliable in areas with complex geological backgrounds. The singularity mapping technique is applicable and useful for extracting local ore-related geochemical anomalies from complicated geochemical backgrounds. Many areas have been predicted to have potential undiscovered Pb mineral deposits in the Qinling region.

Acknowledgements The authors would like to thank the reviewers and editor for critical review of the manuscript and constructive comments.

Funding This work was supported by National Key R&D Program of Deep-penetrating Geochemistry (2016YFC0600600), International Science Cooperation Program of Mapping Chemical Earth: The Belt and Road Geochemical Mapping Project (121201108000150005), and National Nonprofit Institute Research Grant of IGGE (AS2016P02).

References

Afzal, P., Alghalandis, Y.F., Khakzad, A., Moarefvand, P. & Omran, N.R. 2011. Delineation of mineralization zones in porphyry Cu deposits by fractal concentration–volume modeling. *Journal of Geochemical Exploration*, **108**, 220–232.

Agterberg, F.P. 2012. Multifractals and geostatistics. *Journal of Geochemical Exploration*, **122**, 113–122.

Ali, K., Cheng, Q.M. & Chen, Z.J. 2007. Multifractal power spectrum, and singularity analysis for modelling stream sediment geochemical distribution patterns to identify anomalies related to gold mineralization in Yunnan Province, South China. *Geochemistry: Exploration Environment Analysis*, **7**, 293–301, https://doi.org/10.1144/1467-7873/06-116

Arias, M., Gumiel, P. & Martin-Izard, A. 2012. Multifractal analysis of geochemical anomalies: A tool for assessing prospectivity at the SE border of the Ossa Morena Zone, Variscan Massif (Spain). *Journal of Geochemical Exploration*, **122**, 101–112.

Bai, J., Porwal, A., Hart, C., Ford, A. & Yu, L. 2010. Mapping geochemical singularity using multifractal analysis: Application to anomaly definition on stream sediments data from Funin Sheet, Yunnan, China. *Journal of Geochemical Exploration*, **104**, 1–11.

Bölviken, B., Stokke, P.R., Feder, J. & Jössang, T. 1992. The fractal nature of geochemical landscapes. *Journal of Geochemical Exploration*, **43**, 91–109.

Bonham-Carter, G.F. 1994. *Geographic information systems for geoscientists: modelling with GIS, Computer Methods in the Geosciences*. Pergamon, Oxford, New York.

Carranza, E.J.M. 2010. Catchment basin modelling of stream sediment anomalies revisited: incorporation of EDA and fractal analysis. *Geochemistry: Exploration Environment Analysis*, **10**, 365–381, https://doi.org/10.1144/1467-7873/09-224

Chen, Y.J. & Santosh, M. 2014. Triassic tectonics and mineral systems in the Qinling Orogen, central China. *Geological Journal*, **49**, 338–358.

Cheng, Q.M. 1997. Fractal/multifractal modeling and spatial analysis. *In*: Pawlowsky-Glahn, V. (ed.) Proceedings of the international association for mathematical geology (IAMG) conference. Barcelona, Spain, **1**, 57–72.

Cheng, Q.M. 2000. *GeoData Analysis System (GeoDAS) for mineral Exploration: User's Guide and Exercise Manual*. Material for the training workshop on GeoDAS held at York University. 1–3 November, Toronto, Canada.

Cheng, Q.M. 2006. GIS-based multifractal anomaly analysis for prediction of mineralization and mineral deposits. *In:* Harris, J. & Wright, D.F. (eds) *GIS for Geosciences*. Geological Association of Canada, 285–296.

Cheng, Q.M. 2007. Mapping singularities with stream sediment geochemical data for prediction of undiscovered mineral deposits in Gejiu, Yunnan Province, China. *Ore Geology Reviews*, **32**, 314–324.

Cheng, Q.M. 2012. Singularity theory and methods for mapping geochemical anomalies caused by buried sources and for predicting undiscovered mineral deposits in covered areas. *Journal of Geochemical Exploration*, **122**, 55–70.

Cheng, Q.M. & Agterberg, F.P. 2009. Singularity analysis of ore-mineral and toxic trace elements in stream sediments. *Computers & Geosciences*, **35**, 234–244.

Cheng, Q.M., Xu, Y. & Grunsky, E. 2000. Integrated Spatial and Spectrum Method for Geochemical Anomaly Separation. *Natural Resources Research*, **9**, 43–52.

Cohen, D.R., Kelley, D.L., Anand, R. & Coker, W.B. 2010. Major advances in exploration geochemistry, 1998–2007. *Geochemistry: Exploration Environment Analysis*, **10**, 3–16, https://doi.org/10.1144/1467-7873/09-215

Dong, Y.P. & Santosh, M. 2016. Tectonic architecture and multiple orogeny of the Qinling Orogenic Belt, Central China. *Gondwana Research*, **29**, 1–40.

Govett, G.J.S., Goodfellow, W.D., Chapman, R.P. & Chork, C.Y. 1975. Exploration geochemistry—Distribution of elements and recognition of anomalies. *Journal of the International Association for Mathematical Geology*, **7**, 415–446.

Hawkes, E.H. & Webb, J.S. 1962. *Geochemistry in mineral exploration*. Academic Press, New York.

Huang, J. & Hou, L. 2016. Prospecting direction and metallogenic conditions of Pb-Zn deposit in Nanjiang area. *China Manganese Industry*, **34**, 32–37 [in Chinese with English abstract].

Lam, N.S.-N. 1983. Spatial Interpolation Methods: A Review. *The American Cartographer*, **10**, 129–150.

Liu, W., Luo, X.h. & Wang, L.b. 2008. Geological characteristics and genesis of deposit in Guanlinggen Pb-Zn mine. *Gansu Geology*, **17**, 47–53. [in Chinese with English abstract].

Liu, Y., Cheng, Q.M., Xia, Q.L. & Wang, X.Q. 2013. Application of singularity analysis for mineral potential identification using geochemical data - A case study: Nanling W-Sn-Mo polymetallic metallogenic belt, South China. *Journal of Geochemical Exploration*, **134**, 61–72.

Liu, Y., Zhou, K. & Cheng, Q. 2017. A new method for geochemical anomaly separation based on the distribution patterns of singularity indices. *Computers & Geosciences*, **105**, 139–147.

Luz, F., Mateus, A., Matos, J.X. & Gonçalves, M.A. 2014. Cu- and Zn-Soil Anomalies in the NE Border of the South Portuguese Zone (Iberian Variscides, Portugal) Identified by Multifractal and Geostatistical Analyses. *Natural Resources Research*, **23**, 195–215.

Ma, G.L., Beaudoin, G., Qi, S.J. & Li, Y. 2004. Geology and geochemistry of the Changba SEDEX Pb-Zn deposit, Qinling orogenic belt, China. *Mineralium Deposita*, **39**, 380–395.

Mandelbrot, B.B. 1983. *The fractal geometry of nature*. Freeman, San Francisco.

Meng, Q.R. & Zhang, G.W. 2000. Geologic framework and tectonic evolution of the Qinling orogen, central China. *Tectonophysics*, **323**, 183–196.

Miesch, A.T. 1981. Estimation of the geochemical threshold and its statistical significance. *Journal of Geochemical Exploration*, **16**, 49–76.

Rose, A.W., Hawkes, H.E. & Webb, J.S. 1979. *Geochemistry in mineral exploration*. 2nd edn. Academic Press, London.

Sinclair, A.J. 1974. Selection of threshold values in geochemical data using probability graphs. *Journal of Geochemical Exploration*, **3**, 129–149.

Stanley, C.R. & Sinclair, A.J. 1989. Comparison of probability plots and the gap statistic in the selection of thresholds for exploration geochemistry data. *Journal of Geochemical Exploration*, **32**, 355–357.

Sun, X.A., Gong, Q.J., Wang, Q.F., Yang, L.Q., Wang, C.M. & Wang, Z.L. 2010. Application of local singularity model to delineate geochemical anomalies in Xiong'ershan gold and molybdenum ore district, Western Henan province, China. *Journal of Geochemical Exploration*, **107**, 21–29.

Wang, X.Q. & the CGB Sampling Team 2015. China geochemical baselines: Sampling methodology. *Journal of Geochemical Exploration*, **148**, 25–39.

Wang, X.Q., Xu, S.F., Chi, Q.H. & Liu, X.M. 2013*a*. Gold geochemical provinces in China: a micro- and nano-scale formation mechanism. *Acta Geologica Sinica*, **87**, 1–8 [in Chinese with English abstract].

Wang, X.X., Wang, T. & Zhang, C.L. 2013*b*. Neoproterozoic, Paleozoic, and Mesozoic granitoid magmatism in the Qinling Orogen, China: Constraints on orogenic process. *Journal of Asian Earth Sciences*, **31**, 129–151.

Wang, X.Q., Zhang, B.M., Xin, L., Xu, S.F., Yao, W.S. & Ye, R. 2016. Geochemical challenges of diverse regolith-covered terrains for mineral exploration in China. *Ore Geology Reviews*, **73**, 417–431.

Xie, X.J. & Yin, B.C. 1993. Geochemical patterns from local to global. *Journal of Geochemical Exploration*, **47**, 109–129.

Xie, X.J., Mu, X.Z. & Ren, T.X. 1997. Geochemical mapping in China. *Journal of Geochemical Exploration*, **60**, 99–113.

Xie, S.Y., Cheng, Q.M., Chen, G., Chen, Z.J. & Bao, Z.Y. 2007. Application of local singularity in prospecting potential oil/gas Targets. *Nonlinear Processes In Geophysics*, **14**, 1641–1647.

Yang, L., Wang, Q.F., Liu, H., Carranza, E.J.M., Li, G.J. & Zhou, D.Q. 2016. Identification and mapping of geochemical patterns and their significance for regional metallogeny in the southern Sanjiang, China. *Ore Geology Reviews*, https://doi.org/10.1016/j.oregeorev.2016.1008.1014

Ye, R., Wang, X.Q. & Zhang, B.M. 2014. A Microscopic and Nanoscale Understanding of the Formation of Gold Geochemical Provinces. *Acta Geologica Sinica (english Edition)*, **88**, 995–1003.

Zhang, G.W., Meng, Q.R. & Lai, S.C. 1995. Tectonics and structure of Qinling orogenic belt. *Science in China Series B*, **38**, 1379–1394.

Zhao, J.N., Zuo, R.G., Chen, S.Y. & Kreuzer, O.P. 2015. Application of the tectono-geochemistry method to mineral prospectivity mapping: a case study of the Gaosong tin-polymetallic deposit, Gejiu district, SW China. *Ore Geology Reviews*, **71**, 719–734.

Zhou, J.X., Huang, Z.L., Gao, J.G. & Yan, Z.F. 2013. Geological and C–O–S–Pb–Sr isotopic constraints on the origin of the Qingshan carbonate-hosted Pb–Zn deposit, Southwest China. *International Geology Review*, **55**, 904–916.

Zhu, L.M., Zhang, G.W., Guo, B., Lee, B., Gong, H.J. & Wang, F. 2010. Geochemistry of the Jinduicheng Mo-bearing porphyry and deposit, and its implications for the geodynamic setting in East Qinling, P.R. *China. Chemie Der Erde-geochemistry*, **70**, 159–174.

Zimmerman, D., Pavlik, C., Ruggles, A. & Armstrong, M.P. 1999. An Experimental Comparison of Ordinary and Universal Kriging and Inverse Distance Weighting. *Mathematical Geosciences*, **31**, 375–390.

Zuo, R.G. 2014. Identification of weak geochemical anomalies using robust neighborhood statistics coupled with GIS in covered areas. *Journal of Geochemical Exploration*, **136**, 93–101.

Zuo, R.G. & Wang, J. 2016. Fractal/multifractal modeling of geochemical data: A review. *Journal of Geochemical Exploration*, **164**, 33–41.

Zuo, R.G., Cheng, Q.M., Agterberg, F.P. & Xia, Q.L. 2009. Application of singularity mapping technique to identify local anomalies using stream sediment geochemical data, a case study from Gangdese, Tibet, western China. *Journal of Geochemical Exploration*, **101**, 225–235.

Zuo, R.G., Wang, J., Chen, G.X. & Yang, M.G. 2015. Identification of weak anomalies: A multifractal perspective. *Journal of Geochemical Exploration*, **148**, 12–24.